第 32 卷第 8 期 无 机 化 学 学 报 Vol.32 No.8
2016 年 8 月 CHINESE JOURNAL OF INORGANIC CHEMISTRY 1441-1448

聚多巴胺功能化的四氧化三钴纳米复合材料的制备及电催化性能

王海宁 潘伯广 孙 昭 冯涛涛 齐 誉* 洪成林*
(石河子大学化学化工学院,新疆兵团化工绿色过程重点实验室-省部共建
国家重点实验室培育基地,石河子 832003)

摘要: 通过简单的自聚合反应在四氧化三钴表面包覆聚多巴胺膜, 联合使用纳米铂和辣根过氧化物酶用于电催化还原过氧化氢。结果表明,聚多巴胺的使用增强后续纳米铂的负载量和辣根过氧化物酶的生物活性;四氧化三钴、纳米铂和辣根过氧化物酶的多重信号放大作用,大大增强了该复合材料的催化活性,提高了过氧化氢传感器的灵敏度。优化实验条件下,传感器对过氧化氢的检测范围为 0.1~700 μmol·L^{-1},检测限为 0.08 μmol·L^{-1}。

关键词: Co_3O_4; 聚多巴胺; 多重信号放大; 电催化; H_2O_2
中图分类号: TB333 **文献标识码**: A **文章编号**: 1001-4861(2016)08-1441-08
DOI: 10.11862/CJIC.2016.190

Preparation and Electrocatalytic Properties of Polydopamine Functionalized Co_3O_4 Nanocomposite

WANG Hai-Ning PAN Bo-Guang SUN Zhao FENG Tao-Tao QI Yu* HONG Cheng-Lin*
(*School of Chemistry and Chemical Engineering, Key Laboratory of Materials-Oriented Chemical Engineering of Xinjiang Uygur Autonomous Region, Engineering Research Center of Materials-Oriented Chemical Engineering of Xinjiang Bingtuan, Shihezi University, Shihezi, Xinjiang* 832003, *China*)

Abstract: Polydopamine (PDA) bio-functionalized Co_3O_4 nanoparticles (NPs) were successfully synthesised and first applied to the research of electrocatalysis on H_2O_2. Co_3O_4 NPs, as a peroxidase-like, were wrapped with PDA by a simple self-polymerization in mild basic solution. Then, uniformly dispersed platinum nanoparticles (Pt NPs) were deposited on PDA-Co_3O_4. It is found that the introduction of PDA film enhanced the load of Pt NPs, and the combined effect of Co_3O_4, Pt NPs and horseradish peroxidase (HRP) amplified the electrical signal of H_2O_2 sensor. Under optimal conditions, a wide linear detection range from 0.1 to 700 μmol·L^{-1} with a detection limit of 0.08 μmol·L^{-1} was observed.

Keywords: Co_3O_4; polydopamine; multiple signal amplification; electrocatalysis; H_2O_2

0 Introduction

Hydrogen peroxide (H_2O_2), as a kind of commonly used oxidizer and reductant, has been widely used in food industry, clinical diagnostics, pharmacy, environmental monitoring, etc[1-3]. H_2O_2 plays an important role in the living cells depending on the extent, timing, and location of its production. The disorder of H_2O_2 concentration is closely connected with oxidative stress reaction in injury, aging and disease[4]. Therefore, accurately detection for H_2O_2 at low level becomes increasingly important. Electrochemical

收稿日期:2016-03-26。收修改稿日期:2016-06-24。
国家自然科学基金(No.21065009)、教育部重点资助项目(No.210251)和兵团重点领域创新团队计划(No.2015BD003)资助。
*通信联系人。E-mail:hcl_tea@shzu.edu.cn,qy01_tea@shzu.edu.cn

sensors are sensitive and efficient since they can analyze biological sample by direct conversion into an electrical signal[5]. Nanomaterials have stimulated intense research over past decades due to their high biocompatibility and large surface area[6-8].

Metal nanoparticles (NPs) and metallic oxides NPs are increasingly applied in the studies of catalysis, semiconductor, energy storage, and semiconductor as a result of their high surface reaction activity and catalytic activity[9-13]. As a significant transition metal oxide, Co_3O_4 NPs have been reported and applied in catalysis, electrochemical sensors and energy storage[14-17]. Compared with CoO and Co_2O_3, Co_3O_4 exhibit more broad application prospects in electrochemistry because of its extremely high electrocatalytic activity and theoretical specific capacitance[18-19]. Cheng et al. reported that Co_3O_4 directly grown on Ni foam has superior mass transport property, as well as this strategy is low in cost and facile in preparation[20]. Mu et al. reported that Co_3O_4 NPs exhibited peroxidase-like activity and catalase-like activity[21]. However, small molecules like Co_3O_4 nanoparticles usually show poor stability and are easy to aggregate, as a result of the active sites decreased[22-24].

To solve this problem, some research groups wrapped some filming materials around the small molecules, and achieved initial success[24-25]. Liu et al. reported porphyrin functionalized chain-like Co_3O_4 NPs exhibited higher stability and catalytic activity than those of pure Co_3O_4 NPs[23]. Dong et al. reported a novel organic-inorganic hybrid material polypyrrole-Co_3O_4 with good stability was successfully synthesized[26]. Lee et al. reported a very good film-forming biomaterial dopamine[27]. Dopamine, as an important catecholamine neurotransmitter with excellent self-polymerizing ability and biocompatibility, has received great attention on filming material in the past few years[28-29]. The stable polydopamine (PDA) film formed by covalent polymerization and non-covalent self-assembly dopamine is easily linked with many materials such as metallic nanoparticles and biological molecules through the residual catechol groups on the film surface[30-32].

In this paper, we reported the synthesis of PDA bio-functionalized Co_3O_4 NPs and its application in the electrocatalysis on H_2O_2. The Co_3O_4 NPs were covered in PDA film by self-polymerization of dopamine. With the residual catechol groups on the PDA film surface, uniformly dispersed platinum nanoparticles (Pt NPs) could be simply and steadily deposited on PDA-Co_3O_4. Then, the introduction of horseradish peroxidase (HRP) further enhanced the electrocatalytic activity of the nanocomposites. By taking advantages of the excellent biocompatibility, film forming ability of PDA, and high electrocatalytic activity of Co_3O_4 NPs, as well as the combined effect of Co_3O_4, Pt NPs and HRP, the fabricated Co_3O_4-PDA-Pt nanocomposite exhibited excellent electrocatalysis on H_2O_2.

1 Experimental

1.1 Chemicals and materials

Cobaltous nitrate ($Co(NO_3)_2 \cdot 6H_2O$), polyethylene glycol (PEG), butyl alcohol, chloroplatinic acid ($H_2PtCl_6 \cdot 6H_2O$), sodium borohydride ($NaBH_4$), and dopamine were purchased from Alfa Aesar, while horseradish peroxidase (HRP) was from Jianglaibio Co. Ltd. (Shanghai, China). All other chemicals were of analytical grade and used as received without further purification. Phosphate buffer solution (PBS) of various pH values were prepared by mixing the 0.067 $mol \cdot L^{-1}$ stock solutions of KH_2PO_4 and Na_2HPO_4 at specific ratios. All solutions were established with ultrapure water.

1.2 Apparatus

Cyclic voltammetry (CV), electrochemical impedance spectroscopy (EIS) and *I-t* curves were performed using a Potentiostat/Galvanostat Model 283 electrochemical workstation (Ametek, USA). The three-electrode system consisted of a bare or modified gold electrode (GE) which was used as a working electrode, a saturated calomel electrode (SCE) as a reference electrode and a Pt wire counter electrode. The transmission electron microscope (TEM) images were obtained with a H600 transmission electron microscope (Hitachi Instruments, Japan). X-ray powder diffraction

(XRD) measurements were performed on a Bruker D8 advanced X-ray diffractometer with Cu $K\alpha$ irradiation (λ =0.154 06 nm) at 40 kV and 40 mA in the scanning 2θ range of 10° and 90°. Fourier-transform infrared (FT-IR) spectroscopic were determined using a Nicolet Avatar 360 FTIR spectrometer.

1.3 Synthesis of PDA functionalized Co_3O_4 NPs

Co_3O_4 NPs were simply synthesized by hydrothermal method. In brief, 5.0 mL of 1.5 mol·L^{-1} $Co(NO_3)_2$ solution was added into a sample vial. Then, 7.5 mL of 5% (*w*/*w*) PEG and 7.5 mL butyl alcohol were added into the vial with vigorous magnetic stirring. Next, a certain amount of NaOH solution was added into the vial drop by drop and the color of the suspension changed into blue. Then a certain amount of H_2O_2 was dropped slowly and the color further changed into brown-black. The obtained suspension was transferred into a 50 mL Teflon-lined stainless steel autoclave. The autoclave was maintained at 160 ℃ for 10 h after it was tightly sealed. Then, the autoclave was cooled down to room temperature and the black precipitation was washed three times with water and anhydrous ethanol respectively, and then the Co_3O_4 NPs colloid was obtained. The Co_3O_4 NPs colloid was first to be ultrasonically treated for 10 min to ensure Co_3O_4 NPs dispersed in the solution. Subsequently, 40 mL pH 7.0 PBS containing 1.5 mg·mL^{-1} fresh dopamine was added. After that, the solution was violently stirred in ice-water bath for 6 h. Finally, the precipitate was washed with water and then the functionalized Co_3O_4 NPs (Co_3O_4-PDA) were obtained.

The loading of Pt NPs on Co_3O_4-PDA (Co_3O_4-PDA-Pt) was synthesized by in situ deposition. Firstly, the obtained Co_3O_4-PDA solution was dispersed in 4.0 mL of 0.1% (*w*/*w*) H_2PtCl_6 with vigorous magnetic stirring and then 0.1 mL of 0.1 mol·L^{-1} fresh $NaBH_4$ solution was dripped slowly and vigorous stirred for 0.5 h. After centrifugation, the solution was washed with water and then Co_3O_4-PDA-Pt nanocomposite was obtained. For investigating the electrocatalytic properties, Co_3O_4-Pt, PDA-Pt and Co_3O_4-PDA were also prepared by the same method.

1.4 Fabrication of the modified electrodes

10 μL of the Co_3O_4-PDA-Pt suspension was dipped onto the cleaned bare GE surface to dry at 4 ℃ for 4 h. After the Co_3O_4-PDA-Pt modified electrode was dried, 15 μL of 1 mg·mL^{-1} HRP solution was dipped onto the resulting electrode and then it was maintained upon water for 6 h at 4 ℃. Finally, the modified electrode was carefully rinsed with water to remove the physically absorbed HRP, then GE/Co_3O_4-PDA-Pt/HRP was obtained. The schematic representation of the preparation process of GE/Co_3O_4-PDA-Pt/HRP modified electrode is shown in Scheme 1. GE/Co_3O_4, GE/Co_3O_4-Pt, GE/Co_3O_4-PDA/HRP, and GE/PDA-Pt/HRP were also prepared by the same process.

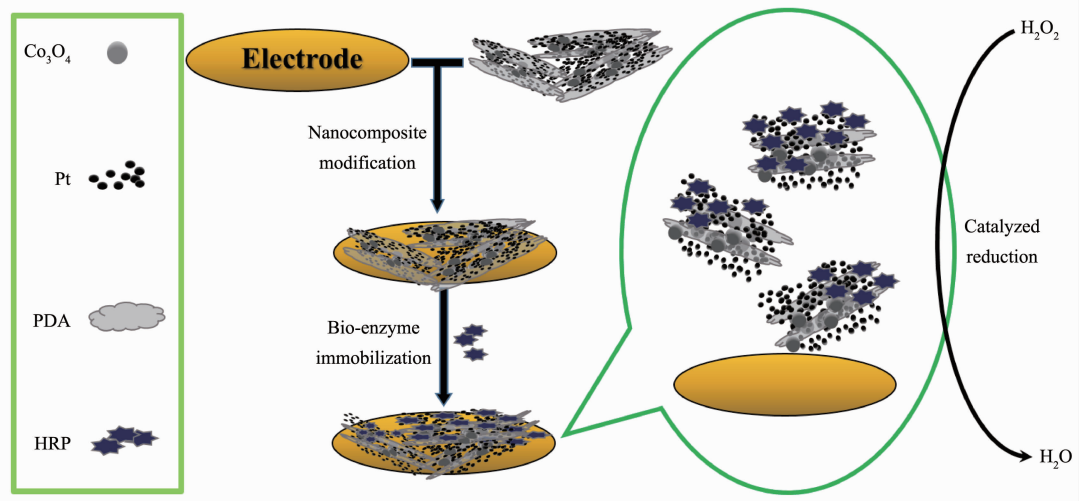

Scheme 1　Schematic representation of the preparation of GE/Co_3O_4-PDA-Pt/HRP

2 Results and discussion

2.1 Characterization of Co_3O_4-PDA-Pt

The morphology and size of Co_3O_4-PDA-Pt nanocomposites were characterized by TEM. Fig.1(a) gives the image of Co_3O_4 NPs. It can be seen that the diameter of them was about 30 nm. Compared with the Co_3O_4 NPs, the diameter of Co_3O_4-PDA increased and obvious layer structure can be seen in Fig.1(b). This indicated that the PDA film was successfully coated on the surface of Co_3O_4 NPs. With the abundant amine groups and residual catechol groups of the PDA film, Pt NPs could be linked simply and steadily on the nanocomposite by *in situ* reduction. As shown in Fig.1(c), a large amount of Pt NPs were uniformly distributed on the Co_3O_4-PDA surface.

The as-synthesised nanocomposites are also determined by XRD and FT-IR. The pattern for the as-prepared Co_3O_4 NPs (Fig.2A(a)) exhibited the diffraction peaks at 2θ =19.01°, 31.34°, 36.91°, 38.73°, 44.90°, 59.55°, 65.36° and 77.22°, which corresponded to (111), (220), (311), (222), (440), (422), (511), (440) and (531) crystal planes and all of which coincided with those for Co_3O_4 cubic (PDF#42-1467, Fig.2A(b)). No impurity peaks were observed, which indicates the high purity of the final products. Fig.2B shows the FT-IR spectra of the as-prepared nanocomposites. As shown in Fig.2B(a), two strong bands at 667 and 565 cm^{-1} appeared, which are assigned to the stretching vibrations of the metal-oxygen bond[33]. The peak at 667 cm^{-1} is attributed to Co-O vibration in tetrahedral hole in which Co is Co^{2+}, and the another peak at 565 cm^{-1} can be attributed to Co-O vibration in octahedral hole in which Co is Co^{3+} [34-35]. This indicated that Co_3O_4 NPs were successfully prepared. Compared with the Co_3O_4 NPs, PDA coated Co_3O_4 NPs showed additional three absorption peaks around 1 296, 1 602 and 3 421 cm^{-1} (Fig.2B(b)). The absorption peaks at 1 296 and 1 602 cm^{-1} are attributed to the C-N stretching vibration and phenylic

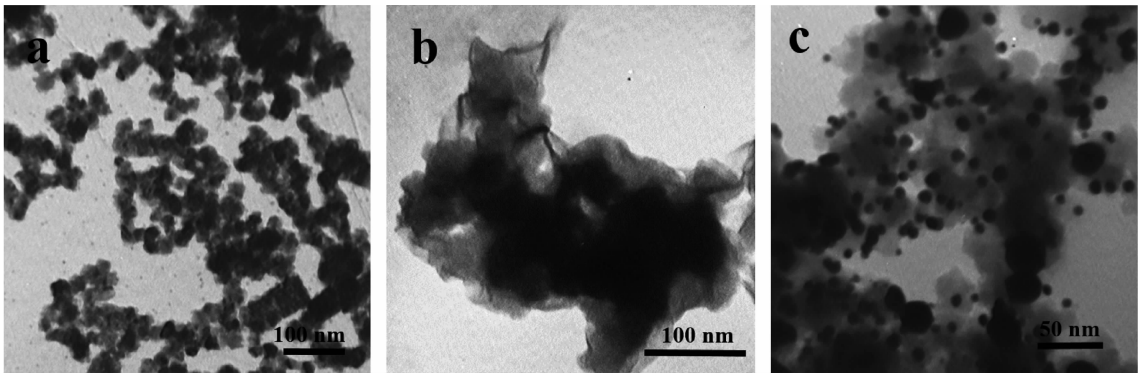

Fig.1 TEM images of Co_3O_4 NPs (a), Co_3O_4-PDA (b) and Co_3O_4-PDA-Pt (c)

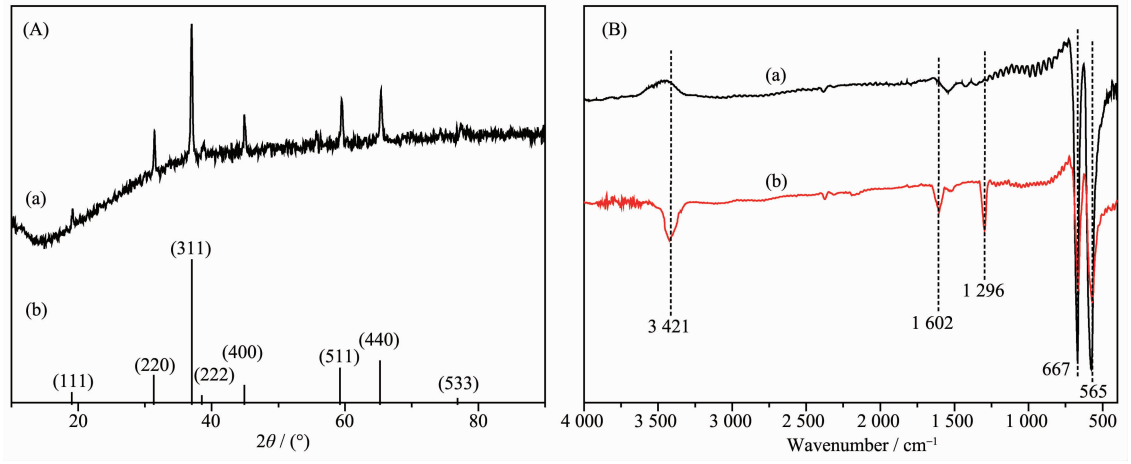

Fig.2 (A) XRD pattern of Co_3O_4 NPs: (a)experimental, (b) PDF#42-1467; (B) FT-IR spectra: (a) Co_3O_4 NPs, (b) Co_3O_4-PDA

C=C stretching vibrations[36-37]. The absorption peaks at 3 421 cm^{-1} is from catechol-OH groups[36].

2.2 Electrochemical characteristics of different modified electrodes

The electrochemical characteristics of different modified electrodes were investigated by cyclic voltammetry (CVs) which was carried out at 50 mV·s^{-1} in 0.067 mol·L^{-1} PBS (pH 7.0) containing 0.1 mol·L^{-1} KCl and 5.0 mmol·L^{-1} $K_3[Fe(CN)_6]$. The CVs of different modified electrodes are shown in Fig.3. As shown in Fig.3a, a pair of well-defined redox peaks corresponding to $K_3[Fe(CN)_6]$ were observed at the bare GE. After the electrode was modified with the Co_3O_4-PDA nanocomposite, the peaks current decreased slightly (Fig.3b), which should be caused by the weak conductivity of PDA. After the Co_3O_4-PDA was loaded with Pt NPs, the Co_3O_4-PDA-Pt modified electrode exhibited a strongly enhancement to redox peaks current, which was mainly from the large surface area and excellent conductivity of Pt NPs (Fig.3c). Compared with Fig.3c, after the adsorption of HRP, the peaks current decreased obviously (Fig.3d), which was mainly from the weak conductivity of macromolecular zymoprotein.

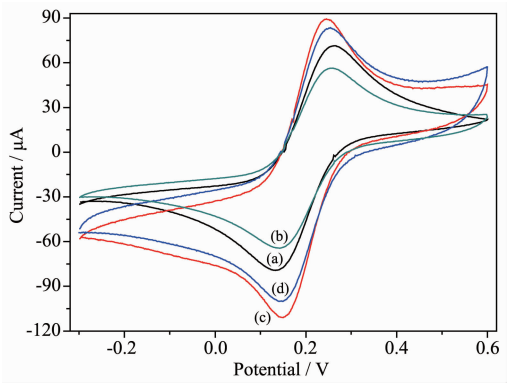

(a) bare GE, (b) GE/Co_3O_4-PDA, (c) GE/Co_3O_4-PDA-Pt, (d) GE/Co_3O_4-PDA-Pt/HRP

Fig.3 CVs of different electrodes at 50 mV·s^{-1} in 0.067 mol·L^{-1} PBS (pH 7.0) containing 0.1 mol·L^{-1} KCl and 5.0 mmol·L^{-1} $K_3[Fe(CN)_6]$

Electrochemical impedance spectroscopy (EIS) can also provide useful information on the impedance changes on the electrode surface during the process of electrodes modification. Fig.4 exhibited the impedance of different modified electrodes in 0.1 mol·L^{-1} KCl solution containing 5.0 mmol·L^{-1} $K_3[Fe(CN)_6]$. As is shown in Fig.4, the Nyquist plot of impedance spectra includes a semicircle portion and a linear portion. The semicircle at high frequency region relates to the electron transfer limited process, and the Warburg linear at low frequencies region relates to the diffusion process[38-39]. The semicircle diameter of EIS spectrum equals to the electron-transfer resistance (R_{et}). It can be seen that the resistance for GE/Co_3O_4-PDA (Fig.4b) was larger than that at bare GE (Fig.4a), which should also be due to the inhibition effect of PDA biopolymer film for electron transfer. Compared with the Co_3O_4-PDA modified electrode, the Co_3O_4-PDA-Pt modified electrode exhibited smaller R_{et} (Fig.4c). The reason might be the enhancer for electron transfer of Pt NPs. When HRP was immobilized onto the GE/Co_3O_4-PDA-Pt surface the resistance of the modified electrode decreased (Fig.4d), which was attributed to the inhibition effect of the enzyme biomacromolecules for electron transfer. The results are also consistent with the previous CVs′ (Fig.3).

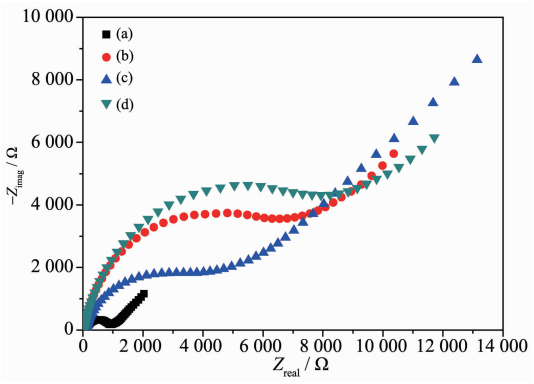

(a) bare GE, (b) GE/Co_3O_4-PDA, (c) GE/Co_3O_4-PDA-Pt, (d) GE/Co_3O_4-PDA-Pt/HRP

Fig.4 EIS of different modified electrodes in 5.0 mmol·L^{-1} $K_3[Fe(CN)_6]$ solution

2.3 Optimization of working potential

The performance of the electrochemical biosensor usually relates to the working potential. Fig.5 showed the current response to successive addition of 10 μmol·L^{-1} H_2O_2 of GE/Co_3O_4-PDA-Pt/HRP at the working potential in the range from 0 to −0.40 V. Curves in Fig.5A display typical current-time curves at different

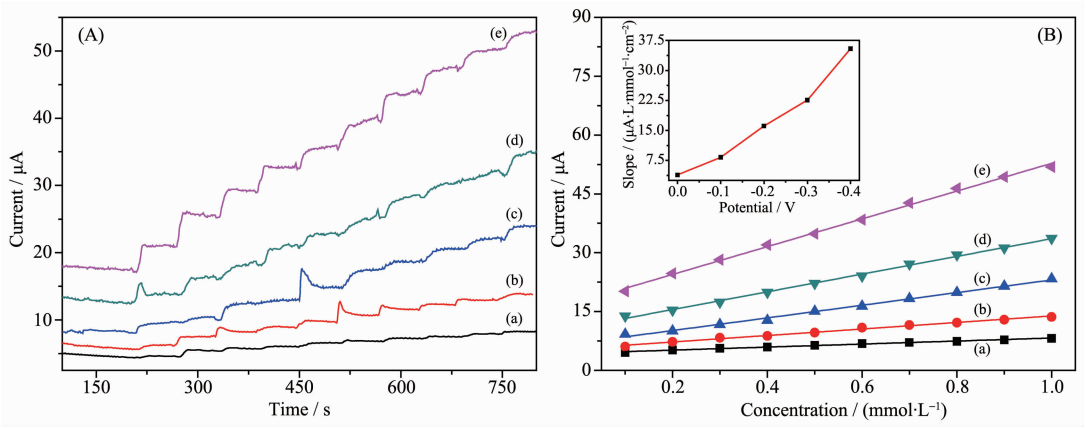

(a) 0 V, (b) −0.10 V, (c) −0.20 V, (d) −0.30 V, (e) −0.40 V; Inset in (B): slope vs working potential curve

Fig.5 Influence of different working potential on current response of GE/Co_3O_4-PDA-Pt/HRP: (A) current–time curves; (B) corresponding calibration curves

working potential for successive addition of 10 μmol·L^{-1} H_2O_2, and the corresponding calibration curves were shown in Fig.5B. Moreover, in order to compare the influence of working potential more clearly, the slope vs working potential curve was presented in the inset of Fig.5B. It was found that the slope continuously increased with the increasing of working potential, and the highest current response appeared at −0.4 V. However, too high working potential results in interference from the matrix species. Therefore, considering the sensitivity of sensor, −0.30 V was chosen for the working potential in the further work.

2.4 Electrocatalytic property towards H_2O_2

To investigate the catalytic activities of different nanocomposites to H_2O_2, different modified electrodes were tested by CV in 0.1 mol·L^{-1} KCl solution containing 5.0 mmol·L^{-1} $K_3[Fe(CN)_6]$ and 10 μmol·L^{-1} H_2O_2 at 50 mV·s^{-1} (Fig.6). Compared with Co_3O_4 NPs modified electrode (Fig.6(a)), Co_3O_4 NPs loaded with Pt NPs modified electrode exhibited larger reduction peak current due to the strong catalytic activity of Pt NPs to H_2O_2 (Fig.6(b)). Fig.6(c) shows that GE/Co_3O_4-PDA-Pt exhibited larger reduction peak current than GE/Co_3O_4-Pt, which might be because the introduction of PDA enhances the load of Pt NPs. Due to the efficient catalytic performance of bio-enzyme, the reduction peak current was further increased after HRP was immobilized onto the GE/Co_3O_4-PDA-Pt surface (Fig.6(d)).

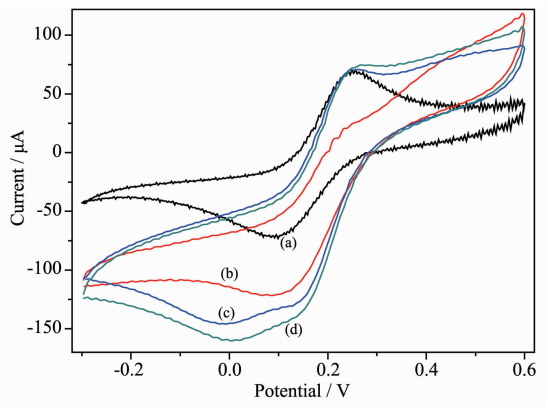

(a) GE/Co_3O_4, (b) GE/Co_3O_4-Pt, (c) GE/Co_3O_4-PDA-Pt, (d) GE/Co_3O_4-PDA-Pt/HRP

Fig.6 CVs of different modified electrodes at 50 mV·s^{-1} in 0.067 mol·L^{-1} PBS (pH 7.0) with 10 μmol·L^{-1} H_2O_2

Comparative experiments were carried out using different modified electrodes by successively adding H_2O_2 to a continuously stirred PBS (pH 7.0) solution at working potential of −0.30 V to further investigate the electrocatalytic properties of Co_3O_4-PDA-Pt nanocomposite (Fig.7). As can be seen, GE/Co_3O_4-PDA-Pt/HRP had the highest current response (Fig.7B(d)). Compared with GE/Co_3O_4-PDA/HRP (Fig.7B(a)) and GE/PDA-Pt/HRP (Fig.7B(b)), the current response of GE/Co_3O_4-PDA-Pt/HRP to H_2O_2 is greatly enhanced, which might be ascribed to the excellent conductivity of Pt NPs. Through this conductivity, Co_3O_4 can play its catalytic role better. Due to the efficient catalytic performance of HRP, the current

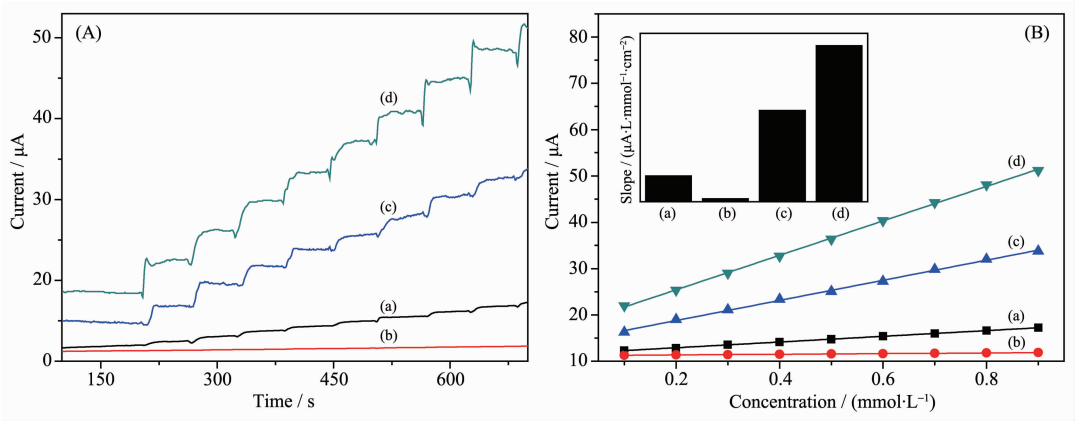

(a) GE/Co_3O_4-PDA/HRP, (b) GE/PDA-Pt/HRP, (c) GE/Co_3O_4-PDA-Pt, (d) GE/Co_3O_4-PDA-Pt/HRP; Working potential: −0.30 V; Inset in (B): slope vs working potential curve

Fig.7　Current response to successive addition of 10 μmol·L^{-1} H_2O_2 of different modified electrodes: (A) current-time curves; (B) corresponding calibration curves

response of GE/Co_3O_4-PDA-Pt/HRP (Fig.7B (d)) was larger than that of GE/Co_3O_4-PDA-Pt (Fig.7B (c)). Based on these results, we confirmed that the combined effect of Co_3O_4, Pt and HRP made the nanocomposite exhibit excellent electrocatalytic properties.

Fig.8 showed the typical current-time curves at GE/Co_3O_4-PDA-Pt/HRP with successive additions of H_2O_2 at −0.30 V. A linear detection range from 0.1 to 700 μmol·L^{-1} with a detection limit (LOD) of 0.08 μmol·L^{-1} was observed. The regression equation is I/μA=2.867×$10^5 c_{H_2O_2}$/(mol·L^{-1})+19.47 (R^2=0.998 2). The GE/Co_3O_4-PDA-Pt/HRP biosensor exhibited higher sensitivity of 1 014.6 μA·L·$mmol^{-1}$·cm^{-2} than those of polyaniline-graphene composited thin film electrode

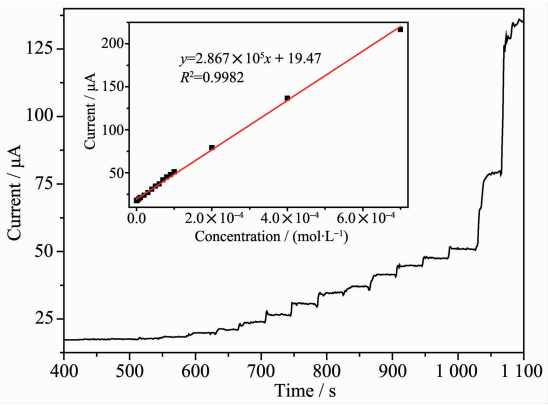

Working potential: −0.30 V; Inset: plot of current vs concentration of H_2O_2

Fig.8　Current response to H_2O_2 additions on GE/Co_3O_4-PDA-Pt/HRP

(325.4 μA·L·$mmol^{-1}$·cm^{-2})[40], hierarchical porous Co_3O_4 electrode (389.7 μA·L·$mmol^{-1}$·cm^{-2})[15] and Pd-TiO_2 electrode (554 μA·L·$mmol^{-1}$·cm^{-2})[41], and nanoporous Ag@BSA/Au electrode (101.3 μA·L·$mmol^{-1}$·cm^{-2})[42]. The results indicated that the fabricated Co_3O_4-PDA-Pt nanocomposite modified electrode H_2O_2 sensor exhibited high sensitivity and wide dynamic measurement range, which mainly due to the high electrocatalytic activity of Co_3O_4 NPs, excellent biocompatibility, film forming ability of PDA and the synergies in Co_3O_4, Pt NPs and HRP.

3　Conclusions

This work reported that PDA bio-functionalized Co_3O_4 NPs were successfully synthesized through a simple and cost-effective strategy and first applied to the research of electrocatalysis on H_2O_2. Co_3O_4 NPs, as a new peroxidase-like, were wrapped with PDA by a simple self-polymerization in mild basic solution. It was found that the introduction of PDA film enhanced the stabilities of Co_3O_4 NPs and Pt NPs and the combined effect of Co_3O_4 and Pt NPs greatly improved the electrocatalytic properties of Co_3O_4-PDA-Pt nanocomposite. The high electrocatalytic activity and stability of the proposed nanocomposite provide potential applications for electrochemical sensors, catalysis, and fuel cells.

Acknowledgements: This work was supported by

Scientific Research Foundation for Changjiang Scholars of Shihezi University, the National Natural Science Foundation of China (Grant No.21065009), Bingtuan Innovation Team in Key Areas (Grant No.2015BD003), and the Key Project of Chinese Ministry of Education (Grant No.210251).

References:

[1] Guo H, Aleyasin H, Dickinson B C, et al. *Cell Biosci.*, **2014**,**4**:1

[2] Kuo C C, Lan W J, Chen C H. *Nanoscale*, **2014**,**6**:334-341

[3] Perathoner S, Centi G. *Top Catal.*, **2005**,**33**:207-224

[4] Van de Bittner G C, Dubikovskaya E A, Bertozzi C R, et al. *Proc. Nat. Acad. Sci. U.S.A.*, **2010**,**107**:21316-21321

[5] Yagati A K, Choi J W. *Electroanalysis*, **2014**,**26**:1259-1276

[6] Liang W, Yi W, Li S, et al. *Clin. Biochem.*, **2009**,**42**:1524-1530

[7] Luo X, Morrin A, Killard A J, et al. *Electroanalysis*, **2006**,**18**:319-326

[8] Chen H, Jiang C, Yu C, et al. *Biosens. Bioelectron.*, **2009**,**24**:3399-3411

[9] Kleijn S E F, Lai S, Koper M, et al. *Angew. Chem. Int. Ed.*, **2014**,**53**:3558-3586

[10]Daniel M C, Astruc D. *Chem. Rev.*, **2004**,**104**:293-346

[11]Guo S, Wang E. *Anal. Chim. Acta*, **2007**,**598**:181-192

[12]Meyer J, Hamwi S, Krger M, et al. *Adv. Mater.*, **2012**,**24**:5408-5427

[13]Kumar D R, Manoj D, Santhanalakshmi J. *Sens. Actuators B*, **2013**,**188**:603-612

[14]Kim H, Park D W, Woo H C, et al. *Appl. Catal., B*, **1998**,**19**:233-243

[15]Han L, Yang D P, Liu A. *Biosens. Bioelectron.*, **2015**,**63**:145-152

[16]Pan L, Zhao H, Shen W, et al. *J. Mater. Chem., A*, **2013**,**1**:7159-7166

[17]Srinivasan V, Weidner J W. *J. Power Sources*, **2002**,**108**:15-20

[18]Cao D, Chao J, Sun L, et al. *J. Power Sources*, **2008**,**179**:87-91

[19]Gao Y, Chen S, Cao D, et al. *J. Power Sources*, **2010**,**195**:1757-1760

[20]Cheng K, Cao D, Yang F, et al. *J. Power Sources*, **2014**,**253**:214-223

[21]Mu J, Wang Y, Zhao M, et al. *Chem. Commun.*, **2012**,**48**:2540-2542

[22]Yang H, Zhang X, Tang A, et al. *Chem. Lett.*, **2004**,**33**:826-827

[23]Liu Q, Zhu R, Du H, et al. *Mater. Sci. Eng. C*, **2014**,**43**:321-329

[24]Hong C, Yuan R, Chai Y, et al. *Electroanalysis*, **2008**,**20**:2185-2191

[25]Sun Z, Luo Z, Gan C, et al. *Biosens. Bioelectron.*, **2014**,**59**:99-105

[26]Dong S, Peng L, Liu D, et al. *Bioelectrochemistry*, **2014**,**98**:87-93

[27]Lee H, Rho J, Messersmith P B. *Adv. Mater.*, **2009**,**21**:431-434

[28]Hong S, Kim K Y, Wook H J, et al. *Nanomedicine*, **2011**,**6**:793-801

[29]Lee H, Dellatore S M, Miller W M, et al. *Science*, **2007**,**318**:426-430

[30]Hong S, Na Y S, Choi S, et al. *Adv. Funct. Mater.*, **2012**,**22**:4711-4717

[31]Wang G, Huang H, Zhang G, et al. *Langmuir*, **2010**,**27**:1224-1231

[32]Wang Y, Liu L, Li M, et al. *Biosens. Bioelectron.*, **2011**,**30**:107-111

[33]Yin J, Cao H, Lu Y. *J. Mater. Chem.*, **2012**,**22**:527-534

[34]Khalaji A D, Fejfarova K, Dusek M, et al. *J. Mol. Struct.*, **2014**,**1071**:6-10

[35]Mu J, Zhang L, Zhao M, et al. *J. Mater. Chem. A*, **2013**,**378**:30-37

[36]Martín M, Salazar P, Villalonga R, et al. *J. Mater. Chem. B*, **2014**,**2**:739-746

[37]Yan L, Bo X, Zhu D, et al. *Talanta*, **2014**,**120**:304-311

[38]Kaar C, Dalkiran B, Erden P E, et al. *Appl. Surf. Sci.*, **2014**, **311**:139-146

[39]Hong C, Yuan R, Chai Y, et al. *Electroanalysis*, **2008**,**20**:989-995

[40]Ameen S, Akhtar M S, Shin H S. *Sens. Actuators B*, **2012**, **173**:177-183

[41]Yi Q, Niu F, Yu W. *Thin Solid Films*, **2011**,**519**:3155-3161

[42]Liu Q, Zhang T, Yu L, et al. *Analyst*, **2013**,**138**:5559-5562